PHYSICAL REVIEW D **74,** 063504 (2006)

Scalar field dark matter: Nonspherical collapse and late-time behavior

Argelia Bernal[1] and F. Siddhartha Guzmán[2]

[1]*Departamento de Física, Centro de Investigación y de Estudios Avanzados del IPN, A.P. 14-740, 07000 México D.F.,MEXICO*

[2]*Instituto de Física y Matemáticas, Universidad Michoacana de San Nicolás de Hidalgo, Edificio C-3, Cd. Universitaria, A. P. 2-82, 58040 Morelia, Michoacán, México*

(Received 24 April 2006; published 7 September 2006)

We show the evolution of nonspherically symmetric balls of a self-gravitating scalar field in the Newtonian regime or equivalently an ideal self-gravitating condensed Bose gas. In order to do so, we use a finite differencing approximation of the Schrödinger-Poisson (SP) system of equations with axial symmetry in cylindrical coordinates. Our results indicate: (i) that spherically symmetric ground state equilibrium configurations are stable against nonspherical perturbations and (ii) that such configurations of the SP system are late-time attractors for nonspherically symmetric initial profiles of the scalar field, which is a generalization of such behavior for spherically symmetric initial profiles. Our system and the boundary conditions used, work as a model of scalar field dark matter collapse after the turnaround point. In such case, we have found that the scalar field overdensities tolerate nonspherical contributions to the profile of the initial fluctuation.

DOI: 10.1103/PhysRevD.74.063504 PACS numbers: 95.35.+d, 04.40.−b, 05.30.Jp, 98.62.Gq

I. INTRODUCTION

Recently, scalar fields have played different roles in several scenarios related to astrophysical phenomena. The reason is that such fields are quite common in theoretical physics, specially branches related to theories beyond the standard model of particles, high dimensional theories of gravity an tensor-scalar theories alternative to General Relativity. In the present research we deal with the scalar field dark matter model (SFDM), which assumes the dark matter to be a classical minimally coupled real scalar field determined by a cosh-like potential. Such potential behaves exponentially at early stages of the universe and as a free field (quadratic potential) at late times, which provides the field with the necessary properties to mimic the behavior and successes of cold dark matter at cosmic scales. In fact in [1–3] it was shown that the mass parameter of the scalar field gets fixed by a desired cut-off of the power spectrum, which has two effects: (i) the theory gets fixed and (ii) there is no overabundance of substructure, which standard cold dark matter cannot achieve. One important consequence is that the boson has to be ultralight with masses around $m \sim 10^{-21,-23}$ eV. This is a substantially important bound, because in the standard dark matter models there are no such ultralight dark matter candidates. The benefit obtained however, is two fold: the scalar field can represent a Bose Condensate of such ultralight particles and the Compton wavelength forbids the scalar field to form cuspy structures. In fact, in [4] it was shown that in order for the scalar field interaction to become long range, the system only needs to be condensed.

After the fluctuation analysis about this candidate and its corresponding concordance with observations—the model mimics the properties of the ΛCDM at cosmic scale—-, the next step has to be in the direction of the study of structure formation and the explanation of local phenomena, like rotation curves in galaxies. Fortunately there have been important advances in such direction [5,6]. About the gravitational collapse, in [7] it was shown that relativistic self-gravitating scalar field configurations can be formed when they have galactic masses provided the mass of the boson is ultralight. Nevertheless, because the gravitational field in galaxies is weak, the race turned into the newtonian limit of the system of equations, which was developed in [8]. The price to be paid is that it is not possible to apply the approach at very early stages of the evolution of the universe, and the profit is that the scalar field in the nonrelativistic regime provides a clear interpretation within the Bose-Condensate formalism and classical Quantum Mechanics. In both cases, the strong gravity and the Newtonian regimes, a wide range of arbitrary spherically symmetric initial configurations collapse and form gravitationally bounded and virialized objects with a smooth density everywhere called oscillatons (except those that are related to unstable initial configurations that collapse into black holes in the strong field regime) [9,10]. This property seems to be fundamental in order to form galactic halos, because several high resolution observations are consistent with regular galactic dark matter profiles in the center of the galaxies [11], which implies that this type of condensate could be an alternative to solve the cuspy density profiles of dark halos.

Two pieces of the model that are in progress are the high energy fully relativistic case, including exponential-like scalar field potentials and the free field weak energy newtonian, both are complementary and necessary to explore the SFDM hypothesis. Inspired in a late-time astrophysical scenario, at stages after the turnaround point where weak field applies and the field is free, the question is whether dark matter halos are gravitationally bounded objects of scalar field which have been formed through a gravitational collapse of initial scalar field overdensities. The newtonian

version of the Einstein-Klein-Gordon system of equations is provided by the Schrödinger-Poisson equations (SP), which are the ones that lead the gravitational collapse of the system. This approximation should work for the evolution of an initial density profile after the epoch when the overdensity fluctuation starts to evolve independently of the cosmic expansion.

In the recent past, it has been found that in spherical symmetry the SP system has equilibrium solutions of two types: stable, for which the wave function is nodeless (called sometimes ground state configurations) and others, for which the wave function has nodes (called sometimes excited configurations) that decay into ground state solutions. From these solutions only the ground state ones are stable [9,12]; even further, it has been found that such configurations behave as late-time attractors for initially quite arbitrary spherically symmetric density profiles [8,13].

In [8] it was shown that free scalar field overdensities after the turnaround virialize and tend to form ground state configurations. Because of a very general scale invariance of the Schrödinger-Poisson system of equations such results were also valid for a structure of arbitrary mass [9]. In [13] was shown that the spherical collapse of SFDM tolerates the introduction of a self-interaction term, which on the other hand is associated to the self-interaction term of a self-gravitating Bose-condensate [14], and helps at allowing diverse sizes and masses of the final configurations.

In this paper we go a step forward and study the collapsing process of nonspherical initial configurations, in particular, those involving at most quadrupolar terms. In order to achieve this goals an axisymmetric code that solves the SP system is needed. We choose to deal with cylindrical coordinates denoted by (x, z), where x is the radial coordinate and z the axial coordinate. The SP system for the free field case in these coordinates reads

$$i\frac{\partial\psi}{\partial t} = -\frac{1}{2}\left(\frac{\partial^2\psi}{\partial x^2} + \frac{1}{x}\frac{\partial\psi}{\partial x} + \frac{\partial^2\psi}{\partial z^2}\right) + U\psi \qquad (1)$$

$$\frac{\partial^2 U}{\partial x^2} + \frac{1}{x}\frac{\partial U}{\partial x} + \frac{\partial^2 U}{\partial z^2} = \psi^*\psi. \qquad (2)$$

where $\hbar = c = 1$ and we are using the rescaled variables $x \to mx$, $z \to mz$, $t \to mt$ and the wave function $\psi \to \sqrt{4\pi G}\psi$. This set of coupled partial differential equations in two spatial dimensions plus time is the core of the present manuscript. As mentioned before, these equations have stable solutions in spherical symmetry (see [13] for solutions also including a nonlinear term in the Schrödinger equation); such solutions have shown to be not only stable, but also late-time attractors for quite arbitrary initial density profiles [9,13]. Therefore, our main task in the present manuscript will be to show that such solutions are still attractors even for nonspherically symmetric initial density profiles.

In the next section we present the code we constructed for the present purpose. In Sec. III we show how a ground state configuration reacts under nonspherical perturbations. In Sec. IV we show the evolution and fate of nonspherical initial density profiles. Finally in Sec. V we draw some conclusions.

II. THE CODE

A. Description

The present code is built under the same numerical finite differences method used in the spherically symmetric case in [9,13]. We approximate the continuous equations (1) and (2) using centered finite differencing for both coordinates x and z on a uniform grid defined by $x = p\Delta x$ and $z = q\Delta z$, p, q integers; we used the same resolution in both directions ($\Delta x = \Delta z$). The spatial differential operator is the same in both equations and we dealt with both in the same manner: aside of the usual finite differencing expression for the space derivatives only two delicate items were included related to the first order derivative with respect to x in (1) and (2): (i) we staggered the grid in the x-direction in order to avoid the divergence of such term and (ii) we transformed such term into $\frac{1}{x}\frac{\partial\psi}{\partial x} = 2\frac{\partial\psi}{\partial x^2}$, with the last expression a derivative with respect to x^2.

1. Schrödinger equation

In the present case this is the evolution equation of the system. We discretize time $t = n\Delta t$, n an integer and Δt the resolution in time. We solve this equation using a second order accurate explicit time integrator, which is a modified version of the usual three steps iterative Crank-Nicholson method [15].

Instead of using a characteristic analysis of the propagating modes to set an open boundary at the edges of the domain, we decided to use a sponge in the outermost region of the domain. The sponge is a concept used successfully in the past when dealing with the Schrödinger equation (for detailed analyses see [9,16]). This technique consists in adding up to the potential in the Schrödinger equation an imaginary potential. The result is that in the region where this takes place there is a sink of particles, and therefore the density of probability approaching this region will be damped out, with which we get the effects of a physically open boundary.

2. Poisson equation

Equation (2) is an elliptic equation for U which we solve using the 2D five-point stencil for the derivatives and a successive over-relaxation (SOR) iterative algorithm with optimal acceleration parameter (see e.g. [17] for details about SOR). In order to impose boundary conditions we made sure the boundaries were far enough for the mass $M = \int |\psi|^2 d^3x$ to be the same along the three faces of the domain and used the monopolar term of the gravitational

field; that is, we used the value $U = -M/r$ along the boundaries with $r = \sqrt{x^2 + z^2}$ for the gravitational potential. At the axis we demanded the gravitational potential to be symmetric with respect to the axis.

B. Construction of equilibrium initial data

Initial data

The nature of the SP system allows one to have plenty of freedom about choosing the initial data, that is: once we choose an initial wave function ψ we integrate (2) at initial time; this means that the initial wave function is quite arbitrary. In fact we implement this type of initial data for the case of nonspherical collapse. Nevertheless, for the purpose of testing our numerical techniques, we decided to use initial data corresponding to spherically symmetric ground state configurations. Here we briefly describe how these data are obtained.

In spherical symmetry Eqs. (1) and (2) read:

$$i\frac{\partial}{\partial t}\psi = -\frac{1}{2r}\frac{\partial^2}{\partial r^2}(r\psi) + U\psi \tag{3}$$

$$\frac{\partial^2}{\partial r^2}(rU) = r\psi\psi^*. \tag{4}$$

where $r = \sqrt{x^2 + z^2}$ is the spherical radial coordinate. It is assumed a time dependence of the type $\psi = \phi(r)e^{i\omega t}$, and demand the conditions of regularity at the origin $\phi(0) = \partial_x\phi(0) = 0$ and isolation $\phi(x \to \infty) = 0$, the system becomes an eigenvalue problem where the frequency of the wave function is the eigenvalue. The system to be solved reads

$$\frac{\partial^2}{\partial r^2}(r\phi) = 2r(U - \omega) \tag{5}$$

$$\frac{\partial^2}{\partial r^2}(rU) = r\phi^2. \tag{6}$$

We use a shooting method that bisects the value of ω for a given central value of ϕ that satisfies the boundary conditions. That is, one constructs a one parameter family of solutions labeled by central field, and a given frequency is found for each value of the label as shown in [9,13]. Excited solutions can be also constructed by allowing ϕ to vanish at a given number of points, but always demanding the satisfaction of the boundary conditions. Up to here the construction in spherical symmetry. Once we account with these data: (i) we interpolated the wave function of the spherical data in the xz-grid and (ii) resolved the Poisson Eq. (2), then we have initial data for ground state configurations in our axially symmetric domain.

The system (3) and (4) is invariant under a clever scaling property given by

$$\{t, r, U, \phi\} \to \{\lambda^{-2}\hat{t}, \lambda^{-1}\hat{r}, \lambda^2\hat{U}, \lambda^2\hat{\phi}\} \tag{7}$$

$$\{\rho, M, K, W\} \to \{\lambda^4\hat{\rho}, \lambda\hat{M}, \lambda^3\hat{K}, \lambda^3\hat{W}\} \tag{8}$$

where U is the gravitational potential, ϕ is the spatial part of the wave function, ρ is the density of probability, M is the integral of ρ, K and W are the expectation value of the kinetic and gravitational energy, respectively, and λ is a scaling parameter. Property (7) and (8) implies that if a solution is found for a given central field value $\hat{\phi}(0) = \hat{\phi}_0$ (e.g. $\hat{\phi}(0) = 1 \Rightarrow \rho(0) = 1$) it is possible to build the whole branch of ground state equilibrium configurations. For instance, if the plot $M vs \rho(0)$ is to be constructed, we know from [9] that for $\hat{\phi}(0) = \hat{\rho}(0) = 1$ we have $\hat{M} = 2.0622$; using the relations (7) and (8) for ϕ and M we find $\lambda = (\rho/\hat{\rho})^{1/4} = M/\hat{M}$, which implies that the desired plot is given by the function $M = 2.0622(\rho(0))^{1/4}$ for all central values of the scalar field density. This function is used later on when showing the attractor behavior of these configurations.

C. Testing the code with ground state configurations

The steps followed in the construction of the solutions to Eqs. (1) and (2) can be summarized as follows: (i) choose a type of initial data for the $t = 0$ slice $\psi(\mathbf{x}, 0)$, (ii) populate the xz grid with those data, (iii) solve Eq. (2) and get a gravitational potential, (iv) using such potential leap the system using (1) a Δt time slice further, (v) use the obtained wave function to solve again (2), (vi) then repeat the loop 4, 5 either until the physics starts going wrong (physical quantities lose convergence, dissipative effects show up) or the cpu-time cannot be afforded.

We test this code using systems whose properties we already know from their construction, these are the ground state equilibrium configurations constructed in the previous subsection; they show a particular property: in the continuum limit the wave function oscillates with constant frequency ω, which implies the density of probability $\rho = |\psi|^2$ and therefore the gravitational potential U remain time-independent. Unfortunately we do not account with infinite resolution and therefore we are solving the discretized versions of Eqs. (1) and (2); instead we solve the second order finite differencing approximation of those equations, which is nothing but a truncated expansion of the solution of the functions involved. Let us describe the situation with an example: assume we start with a ground state configuration with $\psi(\mathbf{0}, 0) = 1$ and therefore the central density $\rho(\mathbf{0}, t) = \rho(\mathbf{0}, 0) = 1$ at all times; first, as we are solving a truncated system of equations the time-independence of the central density cannot be satisfied in a strict fashion, instead we can at most demand the central density to converge to 1 at all times; second, due to the truncation error of the finite differencing we are perturbing the system all the times and therefore the system should behave as an stable configuration that is perturbed and thus should oscillate with the modes obtained from a perturbation theory analysis. Therefore we have a two-fold trap to

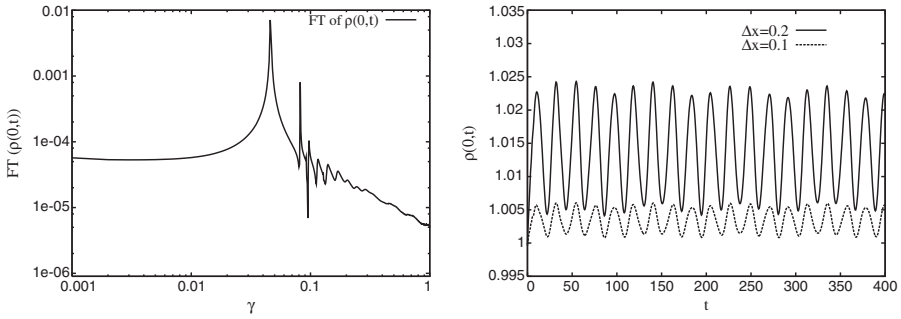

FIG. 1. Left: we show the Fourier transform of the central density of the configuration after the evolution has been performed; the main peak shows up at $\gamma = 0.046$, which coincides with the result found using the perturbation theory in spherical symmetry from [9]. Right: the second order convergence of the central density to the value one is shown using two different resolutions. The runs were carried out on a $x \in [0, 20]$, $z \in [-20, 20]$ domain with resolutions $\Delta x = \Delta z = 0.1, 0.2$. A Cauchy type convergence test decides whether or not we have convergence: the fact that the low resolution run shows a central density 4 times bigger than the one with the double resolution with respect to the value one, indicates the second order convergence to one.

verify whether or not the code is solving the physical system whose properties we know beforehand.

With all this in mind we evolved such a configuration with $\psi(\mathbf{0}, 0) = 1$ with our code and the results are as follows. The Fourier transform in Fig. 1 of the central density reveals that the main frequency of oscillation is $\gamma = 0.046$ which coincides with the result predicted by the first order radial perturbation theory developed in [9]; this indicates that despite the nonspherical nature of our grid, the perturbation due to the discretization of the physical domain is spherical. On the right hand side of Fig. 1 we show the second order convergence of the central density to one, which indicates that our approximations work as they should when we refine the grid and approach the continuum limit.

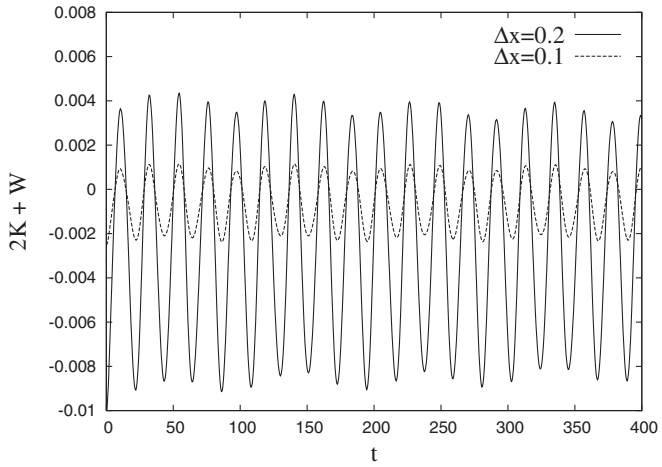

FIG. 2. In this plot we show the meaning of virialized configurations. That is, due to discretization errors when solving the SP equations, there is an intrinsic error in the calculations. We say the system is virialized only in the continuum limit. This is the reason why we show here the second order convergence also for the virial relation. Because this example corresponds to an ground state equilibrium configuration, which we know is virialized, we can be confident that not only the evolution code, but also the diagnostics tools work fine.

In Fig. 2 we verify that ground state equilibrium configurations are virialized in the continuum limit, where the relation $2K + W = 0$ is satisfied with second order convergence. The quantities K and W are calculated as follows:

$$K = -\frac{1}{2}\int \psi^* \nabla^2 \psi d^3x \tag{9}$$

$$W = \frac{1}{2}\int \psi^* U \psi d^3x \tag{10}$$

where the integrations are performed over the numerical domain.

III. NON-SPHERICAL PERTURBATIONS

It is still possible to use the discretization error to perturb a ground state equilibrium configuration in a nonspherical way, for instance, using different resolutions in the x and z directions (see [18] for the use of such trick in relativistic boson stars). However this time we choose to fully-truly perturb the system with the addition of a shell of particles as done in [19], but this time using nonspherical shells like in [20]. We start with a spherically symmetric ground state equilibrium configuration and add up a contribution proportional to a given spherical harmonic. Thus, we propose initial data given by

$$\psi(\mathbf{x}, t) = \psi_{\text{ground}} + \delta\psi \tag{11}$$

where $\delta\psi = e^{-ik_r\sqrt{x^2+y^2}}(\sum_{l=0}^{2} a_l Y_l^0)$, where the coefficients $a_l = A_l e^{-(\sqrt{x^2+z^2}-r_0)^2/\sigma^2}$ are gaussian like shells added to the real part of the wave function of the ground state configuration; on the other hand, the factor $e^{-ik_r\sqrt{x^2+y^2}}$ contributes with a nonzero initial speed of the perturbation; notice that the up labels of the spherical

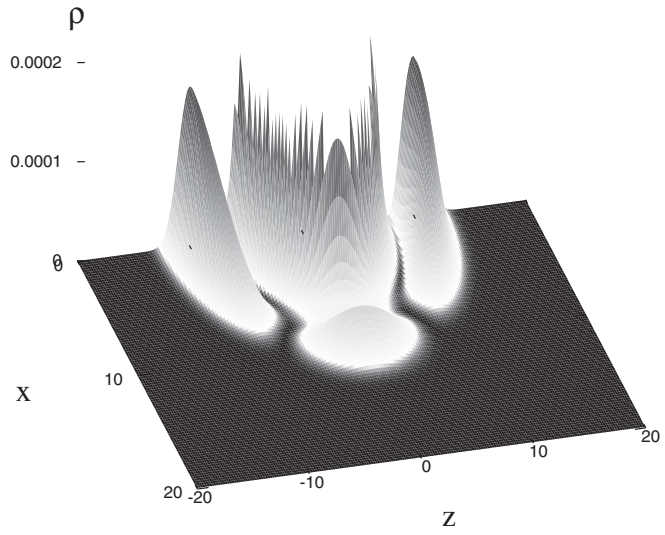

FIG. 3. The initial density profile of the perturbed equilibrium configuration. The central blob corresponds to the equilibrium configuration, whose magnitude is one at the origin. The perturbation thus consists of two blobs coming with speed k_r from the poles and a belt of particles over the equatorial plane.

harmonics are all zero because otherwise they cannot be defined within an axially symmetric grid. Thus the complete set of parameters characterizing the perturbation are: r_0, A_l, σ and k_r.

We practiced several combinations of coefficients a_l, including spherical perturbations containing only the Y_0^0 contribution and found similar results. We only present the one with the parameters: $r_0 = 10.0$, $A_0 = A_1 = 0$, $A_2 = 0.02$, $\sigma = 2.0$, $k_r = -2.0$ carried out on a grid $x \in [0, 20]$, $z \in [-20, 20]$ with resolution $\Delta x = \Delta z = 0.2$. The perturbation shows a quadrupolar contribution. In Fig. 3 we show the density of probability ρ at initial time. The mass of the shell is 0.8% that of the ground state equilibrium configuration.

In Fig. 4 we show the evolution of such system. What can be seen is that the system relaxes and virializes around a spherical ground state equilibrium configuration. The original equilibrium configuration is recovered, which was verified in the following terms: the mass M and the total energy $E = K + W$ approach the values of the equilibrium configuration, the relation $2K + W$ converges to zero in the continuum limit after a short time, the system has a nonspherical initial shape and after a while the ellipticity converges to zero in the continuum limit. This reasons indicate that these ground state equilibrium configurations are stable against nonspherical perturbations that involve the introduction of a quadrupolar shell of particles.

IV. NON-SPHERICAL COLLAPSE

In this section we essay a step forward in the obvious direction, that is, the collapse of nonspherical initial profiles for the SP system of equations. In fact we show that spherically symmetric ground states, are late-time attractors for initial configurations which are not spherically symmetric.

A. Requirements for a nonspherical collapse

The method followed to verify that nonspherical initial configurations evolve toward a spherically symmetric ground state is as follows. (i) Given the evolution of a nonspherical initial profile $\psi(\mathbf{x}, t)$ is carried out, we obtain via a Fourier Transform of a physical quantity, e.g. the central density ρ_c^{ψ}, the frequency γ of the fundamental mode of oscillation of the system; We assume that γ corresponds to the characteristic frequency of oscillation of a linearly perturbed ground state $\psi_{\text{perturbed}}$ toward which ψ is evolving to. This is because the intrinsic perturbation of the system associated to the discretization of the equations, we do not expect that, even for large evolution times, ψ matches exactly a stationary ground state. (ii) Once we estimate f (as done for the construction of Fig. 1) we can calculate the rescaling parameter λ that relates $\psi_{\text{perturbed}}$ and the ground state with $\hat{\psi}(\mathbf{x}, 0) = 1$. Using the definition of frequency and the rescaling relation for t given by (7) the rescaling parameter is calculated as $\lambda = (f/\hat{f})^{1/2}$. (iii) The rescaling parameter λ lets us calculate the nonhat quantities in (8) for the ground state $\psi_{\text{perturbed}}$. Because we are not

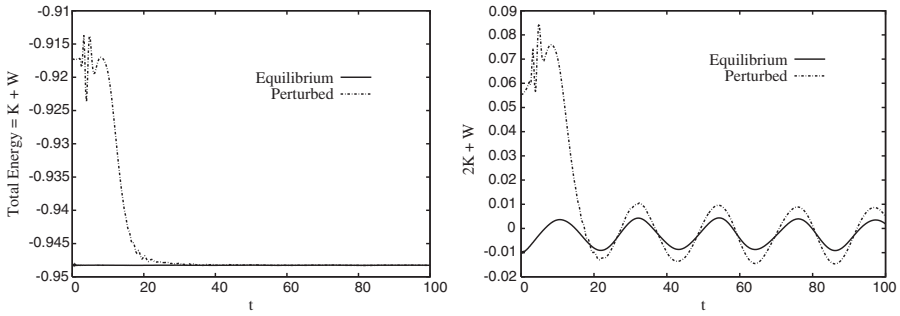

FIG. 4. Left: evolution of the total energy; it can be observed that initially the whole system appears overwarmed due to the presence of the perturbation and its dynamical state; as the time runs, in a rather short time, the system recovers the total energy of the original configuration. Right: the quantity $2K + W$ is monitored and it relaxes and converges to zero with second order.

in the continuum limit we can at most demand that the physical quantities for $\psi(\mathbf{x}, t)$, such as its density ρ_c^ψ and mass M_ψ, converge to those of a ground state configuration. (iv) However, the information related to the convergence to an equilibrium configuration is not enough and we also verify that the fate of ψ is a spherical configuration. We define the ellipticity of the system as the integrated difference between $\rho_z^\psi = \rho(0, z, t)$ and $\rho_x^\psi = \rho(x, 0, t)$ measured from the center of mass of the configuration. We observe for all our nonspherical initial configurations that after a transient period their ellipticity of the system relaxes and becomes zero in the continuum limit. (v) Finally, for all the evolved initial configurations we verify that the virialization condition is satisfied as shown in the perturbation case in Sec. III.

B. Bigger perturbations

In order to illustrate this we show the evolution of a ground state ψ_{ground} plus a considerable nonspherical density contribution which can be already considered to be a nonspherical initial profile. We evolved initial configurations of the form

$$\psi(\mathbf{x}, t) = \psi_{\text{ground}} + \Sigma_{l=0}^{2} a_l Y_l^0 \tag{12}$$

where $a_l = A_l \exp[-r^2/\sigma_l^2]$ is a gaussian with $r = \sqrt{x^2 + z^2}$ centered at the origin, width σ_l and real amplitude A_l. Several runs were made for different A_l and σ_l, and here we present only a representative one. In all cases the result is that the whole system evolves toward a ground state with a mass considerably bigger than that of ψ_{ground} alone. The way in which the system evolves to a ground state is through the gravitational cooling process [9,13], which is powered by the ejection of scalar field.

This attractor behavior has been shown for spherically symmetric configurations in [13] and is shown here for the first time for the case of nonspherical initial profiles. Here we present the results for the initial configuration for which $\psi_{\text{ground}}(\mathbf{0}, 0) = 2$, $l = 1$, $A_l = 1$ and $\sigma_l = 2$. The mass added to the system is the order $\sim 3\%$ that of the original ground state configuration, which implies the following result: some of the added particles joined the ground state configuration and evolved toward another rescaled ground state configuration different from the original one, simply because it is not a small perturbation this time. The evolution was carried out on a grid $x \in [0, 12]$, $z \in [-12, 12]$ with resolutions $\Delta x = \Delta z = 0.1$ and $\Delta x = \Delta z = 0.15$. For this configuration we found the fundamental frequency at late time to be $f = 0.0983$, which gives a rescaling parameter of $\lambda = 1.462$. The central density and mass of the ground state ψ_λ associated with this specific λ are $M_\lambda = 3.014$ and $\rho_c^\lambda = 4.563$. In Fig. 5, we show the evolution of the mass M_ψ versus the central density ρ_c^ψ of the state ψ for the two different resolutions previously specified. The solid line is the branch of all the ground states constructed as indicated in section II and the cross symbol corresponds to the state with the parameters above.

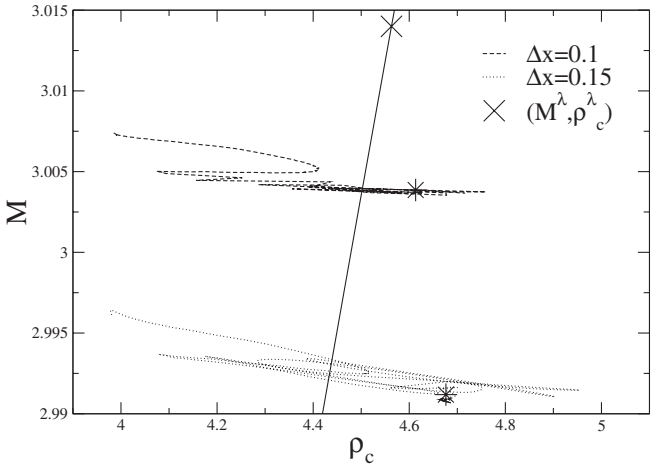

FIG. 5. Evolution of the mass of the initial configuration versus the central density specified in the text. The resolutions used are $\Delta x = \Delta z = 0.1$ (dotted) and $\Delta x = \Delta z = 0.15$ (dashed). The solid line represents the branch of spherical ground states. considering our calculations are second order convergent, from these two runs with the respective resolutions, we infer that the configuration in the continuum limit is that marked with a cross.

Convergence of M_ψ and ρ_c^ψ quantities to the star in the plot is shown also in Fig. 5. The convergence is second order and the stars indicate the configuration we expect the system will relax onto for each resolution. A convergence analysis would reveal second order approach toward the configuration marked with the star. In Fig. 6, we show the ellipticity of the system; we can see that the system relaxes

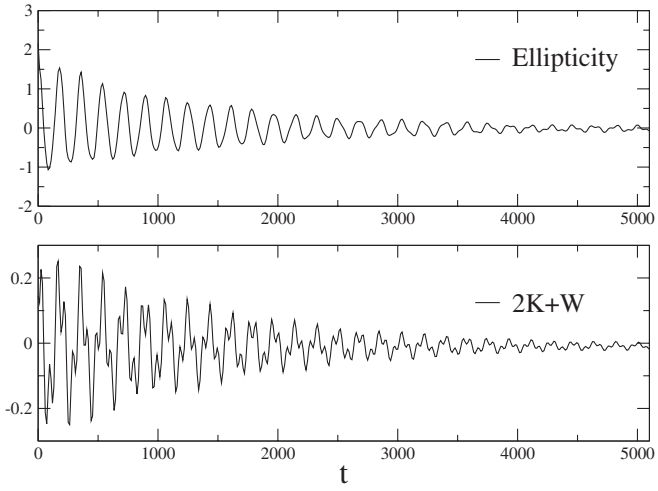

FIG. 6. Evolution of the Ellipticity and the expression $2K + W$. It is shown that after a while the initial axisymmetric configuration evolves toward a spherical one as the Ellipticity goes to zero. On the other hand as $2K + W$ oscillates around zero with decreasing amplitude we conclude that the system tends to a virialized state.

and becomes spherical. Also in this figure it is shown that the system is virialized.

C. Non-Spherical initial profiles

What is in turn is to investigate the evolution of axisymmetric initial configurations. We choose these initial data to have the form

$$\psi(\mathbf{x}, t) = \Sigma_{l=0}^{3} A_l \exp[-r^2/\sigma_l^2] Y_l^0 \qquad (13)$$

where r is as before, σ_l is the width of a gaussian and A_l a real amplitude. Several runs were made for different A_l and σ_l here we present the results for the initial configuration with $A_0 = 9.0$, $A_1 = A_2 = A_3 = 1.0$ and $\sigma_0 = \sigma_1 = \sigma_2 = \sigma_3 = 1.5$. The evolution was carried out on a grid $x \in [0, 12]$, $z \in [-12, 12]$ with resolution $\Delta x = \Delta z = 0.1$ and $\Delta x = \Delta z = 0.15$. For this configuration we found a fundamental frequency $f = 0.128$ that implies a rescaling parameter $\lambda = 1.669$. The central density and mass of the ground state ϕ_λ associated with this specific λ are $M_\lambda = 3.441$ and $\rho_c^\lambda = 7.75$ respectively, a point which is marked with a cross in Fig. 7. In such Figure we show the evolution of the mass M_ψ versus the central density ρ_c^ψ of the state ψ for the two grid resolutions previously specified. The solid line is the branch of all the ground states constructed as indicated in Sec. II. The stars are the configurations the system is approaching to for the different resolutions; because we know such systems are only approximately an equilibrium configuration we practiced a Richardson extrapolation calculation and found that in terms of mass and central density, in the continuum limit -assuming the second order convergence we have in our algorithms- the cross is the configuration these results converge to. Thus in Figs. 7 and 8 we show that the system evolves toward a spherical and virialized configuration.

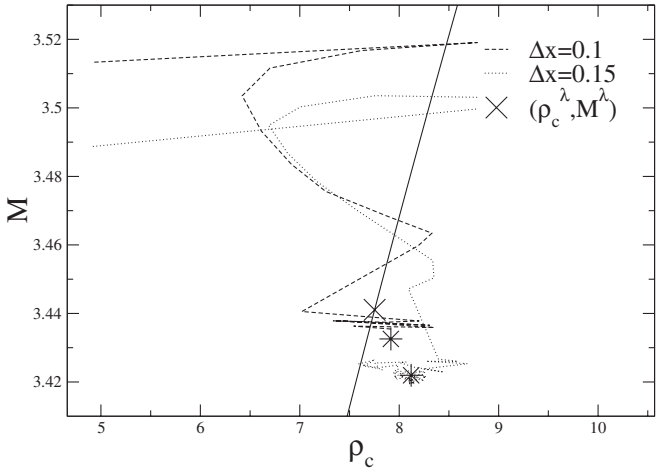

FIG. 7. Evolution of the central density and mass of the initial configuration specified in the text. We used once again resolutions $\Delta x = \Delta z = 0.1$ (dashed) and $\Delta x = \Delta z = 0.15$ (dotted). The solid line represents the branch of spherical ground states. As in the previous subsection, the stars correspond to the states our runs tend to, and the cross indicates the configuration we would achieve with infinite resolution.

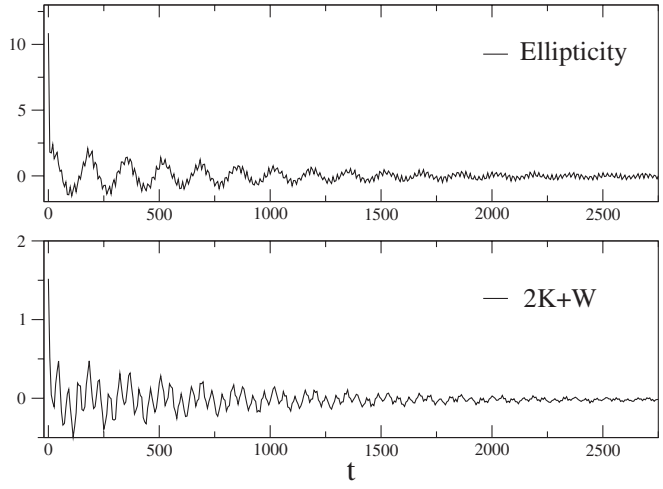

FIG. 8. Temporal evolution of the Ellipticity and the expression $2K + W$ of the initial configuration specified in the text. It is shown that after a while the initial axisymmetric configuration evolves toward a spherical one as the Ellipticity goes to zero. On the other hand as $2K + W$ oscillates around zero with decreasing amplitude we conclude that the system tends to a virialized state.

V. CONCLUSIONS

We have presented a new code designed to solve the SP system with axial symmetry in cylindrical coordinates. We have shown it passes the necessary testbeds of stability and consistency with expected results related to spherically symmetric ground state equilibrium configurations.

We perturbed ground state equilibrium configurations with rather general axially symmetric shells of particles, which were proportional to the first axisymmetric spherical harmonics. Moreover, these shells were endowed with an initial speed toward the equilibrium configuration. The main result is that ground state configurations are stable against this type of perturbations.

Finally, we have evolved axisymmetric initial profiles, and showed that spherically symmetric ground state equilibrium configurations play the role of late-time attractors. This is a generalization of the same result when the initial profiles are spherically symmetric [13]. We have thus shown that the final state of a nonspherical self-gravitating scalar field fluctuation is a ground state spherically symmetric solution. Thus we showed that such configurations are late-time attractors not only for initial spherically symmetric configurations but also for quite general initial axisymmetric shapes.

In the context of the scalar field dark matter model we have quite a new result: the collapse of overdensities tolerates an initial nonspherical contribution to the initial profiles, and moreover, initially axisymmetric profiles tend toward a spherical ground state.

About the process of virialization, with the results at hand we are unable to establish whether the gravitational cooling (powered by the emission of scalar field) is the only responsible for the relaxation of the system. The cases involving a nonzero quadrupolar contribution to the gravitational potential might allow one to formulate the study of another channel, that of the emission of gravitational waves, which would be the subject of a further investigation.

Definitely a major application of the tools shown in this paper is the demonstration of the stability properties of rotating solutions to the SP system of equations constructed in the past [12,21]. It remains unclear whether excited state solutions representing spinning configurations are stable, and whether such solutions could contribute to the SFDM possibilities in terms of quick virialization of collapsed structures and other dynamical properties, for instance, the noncupsy density profile might demand a considerably important spherical contribution in the case the wave function has odd parity.

ACKNOWLEDGMENTS

This research is partly supported by grants PROMEP UMICH-PTC-121 and CIC-UMSNH-4.9. The runs were carried out in the Ek-bek cluster of the "Laboratorio de Supercómputo Astrofísico (LASUMA)" at CINVESTAV-IPN. A. B. acknowledges support from CONACyT.

[1] V. Sahni and L. Wang, Phys. Rev. D **62**, 103517 (2000).
[2] T. Matos and L. A. Ureña-López, Class. Quant. Grav. **17**, L75 (2000).
[3] T. Matos and L. A. Ureña-López, Phys. Rev. D **63**, 063506 (2001).
[4] F. Ferrer and J. A. Grifols, Phys. Rev. D **63**, 025020 (2001).
[5] A. Arbey, J. Lesgourgues, and P. Salati, Phys. Rev. D **64**, 123528 (2001); **65**, 083514 (2002); **68**, 023511 (2003).
[6] J. P. Mbelek, Astron. Astrophys. **424**, 761 (2004).
[7] M. Alcubierre, F. S. Guzmán, T. Matos, D. Núñez, L. A. Ureña-López, and P. Wiederhold, Class. Quant. Grav. **19**, 5017 (2002).
[8] F. S. Guzmán and L. A. Ureña-López, Phys. Rev. D **68**, 024023 (2003).
[9] F. S. Guzmán and L. A. Ureña-López, Phys. Rev. D **69**, 124033 (2004).
[10] M. Alcubierre, R. Becerril, F. S. Guzmán, T. Matos, D. Núñez, and L. A. Ureña-López, Class. Quant. Grav. **20**, 2883 (2003).
[11] S. S. McGaugh, V. C. Rubin, and E. de Block, Astron. J. **122**, 2381 (2001); W. J. G. de Blok, S. S. McGaugh, and V. C. Rubin, Astron. J. **122**, 2396 (2001); G. Gentile *et al.*, Mon. Not. R. Astron. Soc. **351**, 903 (2004)A. D. Bolato, J. D. Simon, A. Leroy, and L. Blotz, Astrophys. J. **565**, 238 (2002).
[12] R. Harrison, I. Moroz, and K. P. Tod, math-ph/0208045.
[13] F. S. Guzmán and L. A. Ureña-López, Astrophys. J. **645**, 814 (2006).
[14] X. Z. Wang, Phys. Rev. D **64**, 124009 (2001).
[15] S. Teukolsky, Phys. Rev. D **61**, 087501 (2001).
[16] M. Israeli and S. A. Orszag, J. Comp. Phys. **41**, 115 (1981).
[17] G. D. Smith, *Numerical Solution of Partial Differential Equations* (Oxford University Press, New York, 1965).
[18] F. S. Guzmán, Phys. Rev. D **70**, 044033 (2004).
[19] J. Balakrishna, E. Seidel, and W-M. Suen, Phys. Rev. D **58**, 104004 (1998).
[20] J. Balakrishna, R. Bondarescu, G. Daues, F. S. Guzmán, and E. Seidel, Class. Quant. Grav. **23**, 2631 (2006).
[21] B. Schupp and J. J. van der Bij, Phys. Lett. B **366**, 85 (1996).